Stellar Photometry of the Globular Cluster NGC 6229. I. Data Reduction and Morphology of the Brighter Part of the CMD

J. Borissova [1]

M. Catelan [2]

N. Spassova [1]

and

A. V. Sweigart [2]

ABSTRACT

BV CCD photometry of the central $(1.5' \times 2.0')$ part of the mildly concentrated outer-halo globular cluster NGC 6229 is presented. The data reduction in such a crowded field was based on a wavelet transform analysis. Our larger dataset extends the previous results by Carney et al. (1991, AJ, 101, 1699) for the outer and less crowded fields of the cluster, and confirms that NGC 6229 has a peculiar color-magnitude diagram for its position in the Galaxy. In particular, NGC 6229's horizontal branch (HB) presents several interesting features, among which stand out: a well populated and very extended blue tail; a rather blue overall morphology, with $(B - R)/(B + V + R) = 0.24 \pm 0.02$; a bimodal color distribution, resembling those found for NGC 1851 and NGC 2808; and gaps on the blue HB. NGC 6229 is the first bimodal-HB cluster to be identified in the Galactic outer halo. A low value of the R parameter is confirmed, suggestive of a low helium abundance or of the presence of a quite substantial population of extreme HB stars fainter than our photometric limit ($\simeq 2.5$ mag below the RR Lyrae level in V). Twelve new possible variable stars were found in the central part of the cluster. The morphology of the red giant branch (RGB) also seems to be peculiar. In particular, the RGB luminosity function "bump" is not a prominent feature and has only been tentatively identified, on the basis of a comparison with a previously reported detection for M3 (NGC 5272). Finally, we compare the properties of NGC 6229 with those for other outer-halo globular clusters, and call attention to what appears to be a bimodal HB distribution for the outer-halo cluster population, where objects with very red *or* very blue HB types are much more frequently found than clusters with intermediate HB types.

[1] Institute of Astronomy, Bulgarian Academy of Sciences, 72 Tsarigradsko chaussèe, BG – 1784 Sofia, Bulgaria

[2] NASA/Goddard Space Flight Center, Code 681, Greenbelt, MD 20771, USA

Subject headings: Stars: Hertzsprung-Russell (HR) diagram — Stars: Horizontal-Branch — Stars: Population II — Globular clusters: individual: NGC 6229.

1. Introduction

The globular cluster (GC) NGC 6229 (C1645+476) is one of the most remote objects associated with the Galaxy, lying about 28 kpc from the Galactic center (Harris 1996). The first color-magnitude diagram (CMD) for this low-reddening $[E(B-V) \simeq 0.01$ mag; Harris 1996] cluster was presented by Cohen (1986), who suggested that the horizontal branch (HB) of NGC 6229 is unusually red for its metallicity ([Fe/H] $= -1.44$; Harris 1996). Subsequently, Carney et al. (1991, hereinafter CFT91) obtained extensive BV CCD photometry for the brighter part of the CMD of NGC 6229. In their survey, CFT91 investigated the external regions of the cluster beyond $0.8'$ from the cluster center. In contrast with the results by Cohen, they detected a substantial blue HB population, suggesting that the HB of NGC 6229 is instead quite bluer than the average for the outer-halo globulars, where substantially well-populated extended blue HBs are not usually found. The available data also suggest a relative paucity of RR Lyrae variables in comparison with both the blue and red HB stars in this cluster. A similar effect seems to be present in the strongly bimodal-HB clusters NGC 2808 (Ferraro et al. 1990) and NGC 1851 (Walker 1992; Saviane et al. 1996). An explanation for the origin of the bimodal HB distributions in these clusters is expected to have a major impact upon our understanding of the second-parameter phenomenon (e.g., Rood et al. 1993; Stetson et al. 1996). For these reasons, it is especially important to increase the number of HB stars in the CMD of NGC 6229.

This paper presents the first CCD photometry of the central $(1.5' \times 2.0')$ region of NGC 6229 performed in Johnson's (BV) photometric system. In Sect. 2, we describe our observations and explain the adopted non-standard data reduction procedure; an analysis of the errors is given in Sect. 3; the red giant branch (RGB) is described and discussed in Sect. 4; the morphology of NGC 6229's HB is addressed in Sect. 5; the existence of radial population gradients is discussed in Sect. 6; and, finally, in Sect. 7 the characteristics of NGC 6229 are compared with those for other outer-halo clusters. In a subsequent paper (Catelan et al. 1996), we shall present a theoretical analysis of the CMD morphology of this cluster, with particular emphasis on the reproduction of its HB morphology by means of synthetic models based upon the latest evolutionary prescriptions for HB stars and RR Lyrae variables.

2. Observations and data reduction

2.1. Observations

The observations of NGC 6229 were obtained with the 2m Ritchey–Chrétien telescope of the Bulgarian National Astronomical Observatory. A set of CCD frames in the BV system was taken with the SBIG Model ST−6 camera. The detector size is 375×242 pixels, the scale is $0.30'' \times 0.34''$ per pixel and the image size is about $1.5' \times 2.0'$. This camera was kindly granted by the EAS/ESO program in support of astronomy in the Central/Eastern Europe countries.

Exposure times ranged from 300 to 900 s in V and from 900 to 1200 s in B.

During the nights of the observations, the seeing was stable with a measured stellar point-spread function (PSF) on the raw frames of about $0.8''$ FWHM. The mean airmass over the duration of each exposure was between 1.1 and 1.2.

2.2. Wavelet transform analysis

The preliminary reductions of the CCD frames, including bias subtraction and flat fielding, were carried out using the standard IRAF data reduction package.

In the central part of such a concentrated cluster as NGC 6229 ($c \simeq 1.61$; Trager et al. 1993), crowding prevented accurate photometry from being obtained. However, by using the positions of stars determined from frames after noise suppression using a wavelet transform analysis, we were able to obtain reasonable photometry at and above the HB level. Similar techniques had previously been employed by other authors (e.g., Aurière & Coupinot 1989) to obtain improved photometric data for stars in the dense fields that characterize concentrated GCs.

As described by Coupinot et al. (1992), the wavelet transform can be regarded as a set of "filters" using a numerical mask with a varying size. It leads to the decomposition of the image into a set of maps exhibiting structures at certain scales. In the present application, we used the method to detect and localize unresolved stars in the core of NGC 6229. We assumed that both the input images and the PSF can be characterized by gaussian profiles in order to fit better the seeing-induced core of the stellar image.

Following the method described by Murtagh et al. (1995), we carried out a discrete convolution of the image using a filter based on the B_3 spline interpolation. The 5×5 mask was used. The hypothesis of a white gaussian noise was adopted to determine the noise of the image. By means of the standard photometric package DAOPHOT (Stetson 1987), we were then able to determine the positions of the stars on the resolved image.

2.3. Numerical simulations

In order to check the position accuracy, a set of numerical simulations was carried out. The first such simulation involved stellar objects in a non-crowded field. In this experiment, 10 different sets of 500 randomly placed point sources and a gaussian background were laid out in a grid of 375×242 pixels. The magnitudes of the point sources were random values ranging from 15 to 20 mag. The PSF was a gaussian function with a FWHM equal to 3 pixels. After wavelet transforming the test images, the DAOPHOT fitting package was used to determine the positions of the point sources in the "original" and "resolved" images. The mean differences between the positions of the point sources in the "original" and "resolved" images are $\Delta X = 0.002$ ($\sigma = 0.015$)

TABLE 1. Gain in efficiency using the wavelet method as a function of the concentration parameter c.

c	N_{org}	N_{dao}	N_{wav}	Gain (%)
0.0	5000	4480	4580	2.0
0.5	5000	4040	4440	8.0
1.0	5000	3560	4345	15.7
1.5	5000	2620	4250	32.6
2.0	5000	1720	2575	17.1

and $\Delta Y = 0.005$ ($\sigma = 0.016$) in X and Y pixel coordinates, respectively.

A second simulation was made for stellar objects in a crowded field. We built test images with the same characteristics as described above, but added a "concentration" parameter equivalent to King's (1966) concentration parameter c. In this case, we assume $c = 1.6$. The mean differences are $\Delta X = 0.01$ ($\sigma = 0.16$) and $\Delta Y = 0.04$ ($\sigma = 0.16$) in X and Y coordinates, respectively.

A third simulation was made in order to test the efficiency of the wavelet method as a function of the degree of central concentration. For this purpose, some test images were built with different concentration parameters c, again assuming a random distribution of magnitudes between 15 and 20 mag. Table 1 summarizes the results. The entries in Table 1 are as follows: c is the concentration parameter, ranging from 0 (randomly placed point sources) to 2 (highly concentrated cluster); N_{org} is the number of point sources placed on the "original" frame; N_{dao} is the number of point sources determined by DAOPHOT on the "original" frame; and N_{wav} is the number of point sources determined by DAOPHOT on the "resolved" (wavelet-transformed) image. The last column shows the gain in efficiency, defined as Gain $= (N_{\mathrm{wav}} - N_{\mathrm{dao}})/N_{\mathrm{org}}$, obtained by using the wavelet transform method. The method is clearly most useful for medium crowded fields, and our tests show that this is the case over the entire range of magnitudes.

One final test was carried out in order to see how the efficiency of the method depends on the magnitudes of the sources. We prepared several test images with point sources of equal magnitudes: 15, 16, 17, 18, 19, and 20 mag. The concentration parameter adopted was $c = 1.5$. Table 2 lists the results of this experiment. In column 1, the magnitude m is indicated. The

TABLE 2. Gain in efficiency using the wavelet method as a function of the magnitude m.

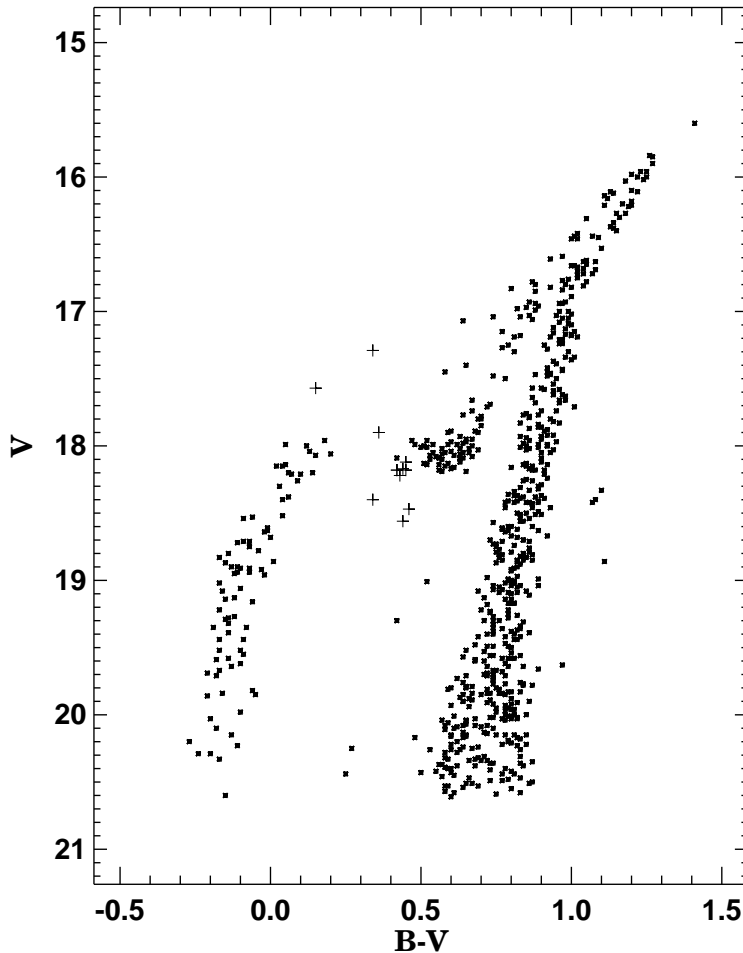| m	N_{org}	N_{dao}	N_{wav}	Gain (%)
15.0	5000	3335	4815	29.6
16.0	5000	3100	4010	18.2
17.0	5000	3010	3590	11.6
18.0	5000	3180	3510	6.6
19.0	5000	2910	3180	5.4
20.0	5000	3000	3250	5.0

Fig. 1.— The observed V vs. $B-V$ CMD for the central regions of NGC 6229 derived from this work. The new candidate RR Lyrae variable stars are shown as plus signs. The 7 RR Lyrae variables which are known to be present in the field have not been plotted.

remaining columns have the same meanings as in Table 1.

Based on the above tests we can conclude that the wavelet transform technique is a rather powerful method for analyzing the photometric data in crowded fields.

2.4. CMD

The photometry of the stars on the frames was performed by means of the PSF fitting package DAOPHOT using a list of X, Y coordinates determined from the "resolved" images.

The instrumental values were corrected for extinction and transformed to the standard
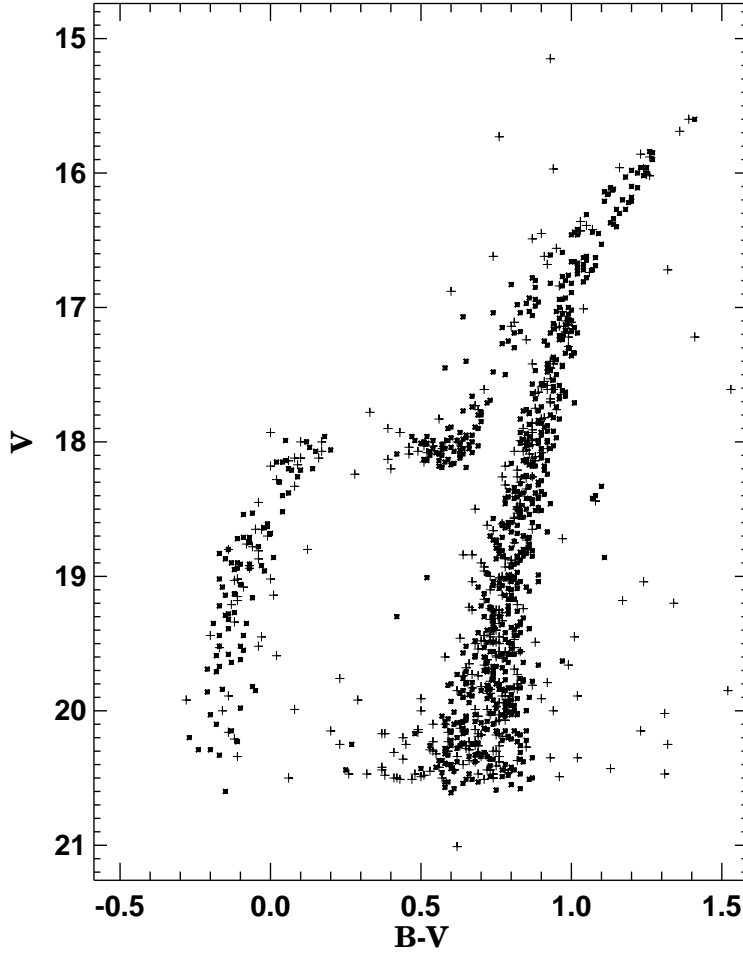
Fig. 2.— The composite CMD of NGC 6229 based on our CCD data ($\times$) and the data of CFT91 (+). Known and candidate RR Lyrae variables have been omitted.

BV system using a technique similar to that described by Christian & Heasley (1988). The instrumental b and v magnitudes were converted to the standard B and V system by means of the equations:

$$V = v + 2.806 - 0.301\,X + 0.011\,(b - v),$$
$$B - V = -0.629 - 0.123\,X + 1.022\,(b - v),$$

where X represents the airmass. The coefficients were determined by reducing the frames of the standard fields in NGC 7006 (Christian et al. 1985) using an aperture photometry algorithm. The rms deviations of the reduced CCD photometry from the standard values are 0.012 mag in V and 0.015 mag in B, over the range of the standards.
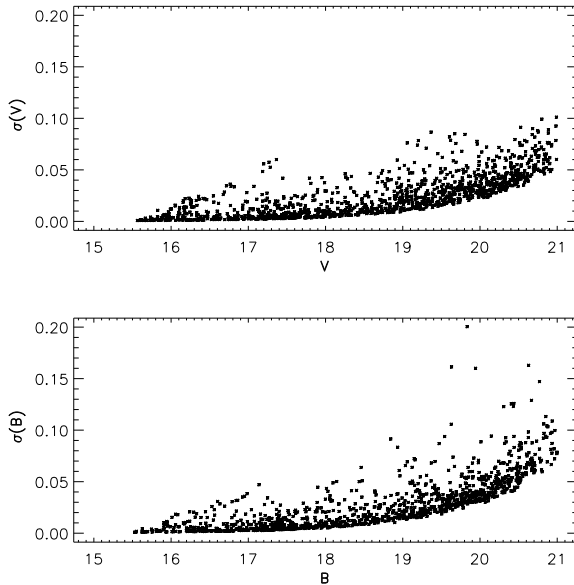
Fig. 3.— Internal errors of the CCD photometry. The rms values σ of the frame-to-frame scatter in the magnitudes V and B are plotted for each star as a function of V (upper panel) or B (lower panel).

Our final photometric list contains 700 stars in the central $1.5' \times 2.0'$ field of NGC 6229. Data are available by E-mail request to the first author. In Fig. 1, we show the CMD obtained from the present investigation. New candidate RR Lyrae variables are shown as plus signs (cf. Sect. 5.1).

As already stated, CFT91 investigated the more external regions of the cluster beyond $0.8'$ from the cluster center, while our CMD covers the core region. We have transformed our coordinates and magnitudes to the coordinate and magnitude system of CFT91 using 60 stars in common between the two studies. We then added the 400 external stars by CFT91 to our internal list of 700 stars in order to generate a common list of stars and produce the combined CMD that is displayed in Fig. 2. Known or suspected RR Lyrae variables have not been included in this plot.

3. Error analysis

3.1. Photometric errors

In order to evaluate the internal accuracy of our CCD measurements, we have used the procedure described by Buonanno et al. (1995). The instrumental magnitudes obtained for each frame were adjusted to a common reference level and averaged for the final calibration. The rms values were computed according to the formula given by Buonanno et al.
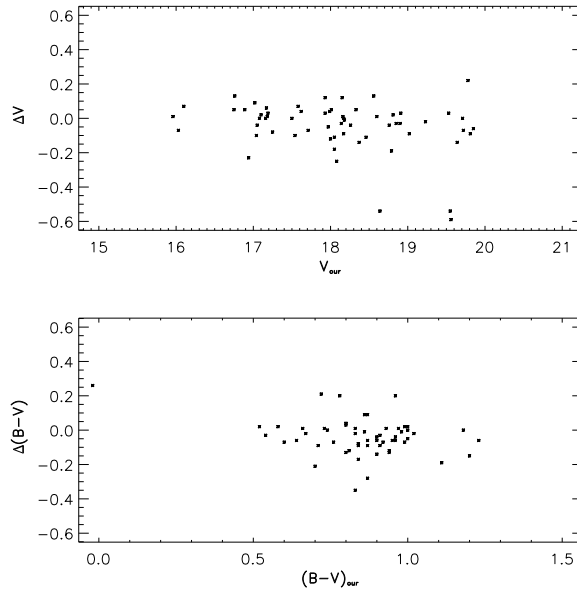
Fig. 4.— Comparison of the V magnitudes (upper panel) and $B-V$ colors (lower panel) derived here with the photometry of CFT91. The comparison is in the sense of this work minus CFT91.

The results for each star in the B and V filters are plotted in Fig. 3 as a function of the final adopted magnitude. These internal errors were averaged over the stars in different magnitude intervals to give the following mean errors: $\epsilon_V = 0.008$ and $\epsilon_B = 0.009$ for $15.50 < V(\mathrm{mag}) < 19.50$, and $\epsilon_V = 0.03$ and $\epsilon_B = 0.038$ for $19.50 < V(\mathrm{mag}) < 21.00$, where the errors are expressed in magnitudes.

3.2. Comparison with CFT91

We have compared our data with the photometry of CFT91 in order to check for any systematic effects. The residuals in the measurements of stars in common between the two studies are plotted in Fig. 4 as a function of the magnitudes and colors derived in the present investigation. Inspection of these diagrams reveals no systematic trend in the V magnitudes. There is, however, a small systematic color shift $[\Delta(B-V) = -0.02]$, with our photometry being a little redder than the photometry of CFT91.

3.3. Field star contamination

It is obviously necessary to check for field star contamination before discussing the detailed structure of the cluster's CMD. Based on the Bahcall & Soneira (1980) model of the Galaxy,

TABLE 3. Expected numbers of field stars towards NGC 6229.

Color range	$14 < V < 16$	$16 < V < 18$	$18 < V < 20$	$20 < V < 22$
$B - V < 0.8$	0.108	0.207	0.300	0.690
$0.8 < B - V < 1.3$	0.042	0.186	0.294	0.267
$B - V > 1.3$	0.009	0.045	0.267	0.087
Total	0.159	0.438	0.861	1.044

Ratnatunga & Bahcall (1985) have predicted field star densities in the direction of NGC 6229. Table 3 gives the number of objects expected per bin of magnitude and color in the area covered by our observations. As one can easily see, field stars should not seriously affect the structure of the CMD.

3.4. Completeness

To determine the completeness function, artificial star experiments are usually carried out (Mateo 1988; Stetson & Harris 1988; Stetson 1991a). In the present case, 10 different sets of 100 randomly placed stars were added to the "original" B and V frames. The frames were "resolved" by means of the wavelet transform (cf. Sect. 2) and the resulting images were then re-reduced. Since completeness is a function of the distance from the cluster center and of the limiting magnitude, we performed the procedure in three radial annuli with $r < 0.26'$, $0.26' < r < 0.46'$ and $0.46' < r < 1.13'$. Fig. 5 shows the completeness functions in the different annuli plotted as a function of the B and V magnitudes. As can be seen, the CMD becomes severely incomplete for $V \gtrsim 19.5$ mag for the innermost zone, $V \gtrsim 20.0$ mag for the intermediate zone, and $V \gtrsim 20.5$ mag for the outer zone of the cluster. For this reason, we cannot rule out the possibility that the blue HB of NGC 6229 is actually more extended than shown in Figs. 1 and 2. This possibility will be discussed further in Sect. 5.4.

We turn now to an analysis of the NGC 6229 CMD.

4. RGB morphology

In Fig. 6, we superimpose the M3 (NGC 5272) ridgeline (Buonanno et al. 1994) on the CMD of NGC 6229 from Fig. 2. In producing this plot, we have adjusted the M3 ridgeline to the NGC 6229 distance, which was achieved by forcing the two HBs to coincide at the RR Lyrae level (implying a $\delta V = 2.42$ mag shift), and have also taken into account a small, but possible, reddening difference between the two clusters $[\delta E(B-V)_{\mathrm{NGC\,6229-M3}} = 0.01$ mag$]$.
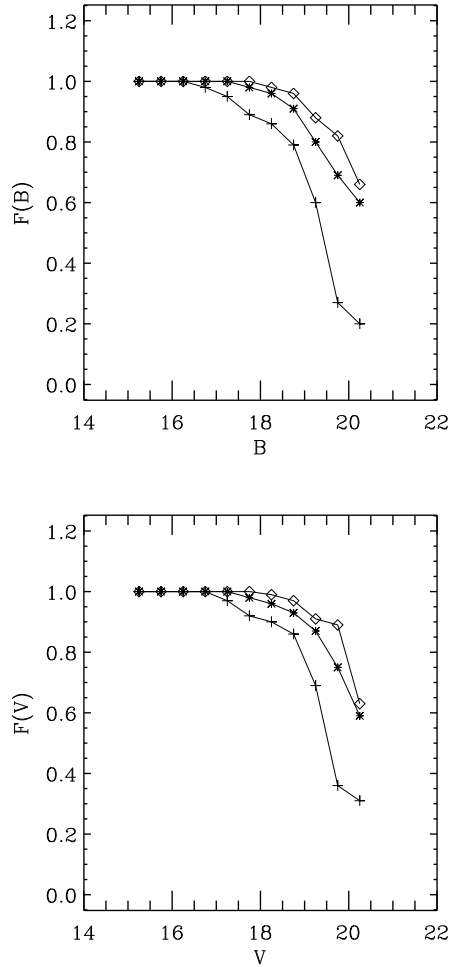
Fig. 5.— Completeness curves in B (upper panel) and V (lower panel) for annuli located at different distances from the cluster center (+: $r < 0.26'$; *: $0.26' < r < 0.46'$; ◇: $0.46' < r < 1.13'$).

The two clusters have quite comparable metallicities, with $[\mathrm{Fe/H}]_{\mathrm{M3}} = -1.57$ (Harris 1996) or possibly slightly higher (Kraft et al. 1992; Carretta & Gratton 1996; Ferraro et al. 1996). As expected for similar metallicity clusters, the slopes of the upper RGBs ($V \lesssim 17$ mag) are quite similar. However, in the range $17 \lesssim V(\mathrm{mag}) \lesssim 19$ there is a discrepancy, with the M3 RGB being significantly hotter. This same discrepancy is also present in the photometric data given in Table 3 of CFT91. We do not have a good explanation for this problem. If, however, combined metallicity and reddening effects were involved, one would then not expect the upper RGBs of the two clusters to coincide. Another unusual feature of the NGC 6229 RGB is an abrupt change in slope at $(V, B-V) \simeq (16.9, 1.0)$.

We have attempted to apply the Fusi Pecci et al. (1990) procedure to locate the RGB luminosity function "bump" in NGC 6229. The purpose of their technique is to identify the
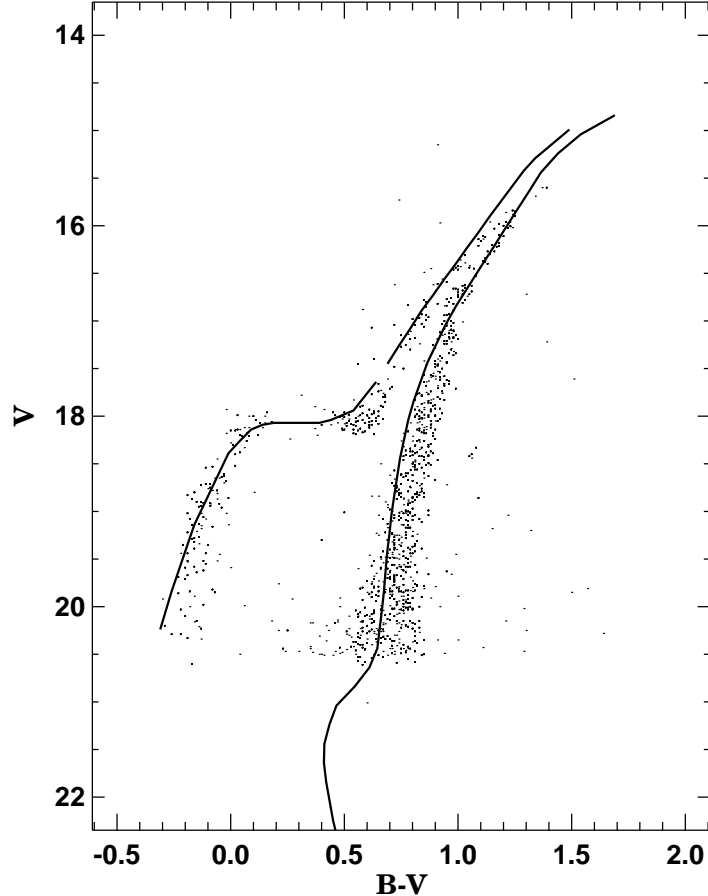
Fig. 6.— Same as Fig. 2, but with the M3 ridgelines from Buonanno et al. (1994) superimposed on the CMD. Shifts in the latter have been applied both in V ($\delta V = 2.42$ mag) and in $B-V$ [$\delta(B-V) = 0.01$ mag], so as to account for the differences in distance modulus and reddening between the two clusters.

break in the slope of the cumulative RGB luminosity function which occurs when the H-burning shell reaches the discontinuity in the H abundance profile that was caused by the previous deep penetration of the convective envelope during the first dredge up. The RGB luminosity function for NGC 6229, plotted in Fig. 7, tentatively suggests that this break in the slope coincides with a feature in the differential luminosity function, at $V \simeq 18.05 \pm 0.07$, which resembles very closely (both in sharpness and location) the feature in the M3 luminosity function that Fusi Pecci et al. have associated to the bump in that cluster (cf. their Figs. 3 and 4). From Eq. (7) in Fusi Pecci et al., assuming [Fe/H] $= -1.44$ and [α/Fe] $= 0$ for the cluster, we would expect the bump to be present at ≈ 0.1 mag above the lower envelope of the HB. Since the lower envelope of the HB is at $V(\mathrm{HB}) \simeq 18.20 \pm 0.03$ mag, we derive $\Delta V(\mathrm{bump} - \mathrm{HB}) \simeq -0.10 \pm 0.08$. Our results are thus in good agreement with those presented by Fusi Pecci et al. for their sample of clusters, *if* the noted feature proves indeed to be the RGB bump. We note, however, that the tentative NGC 6229 bump
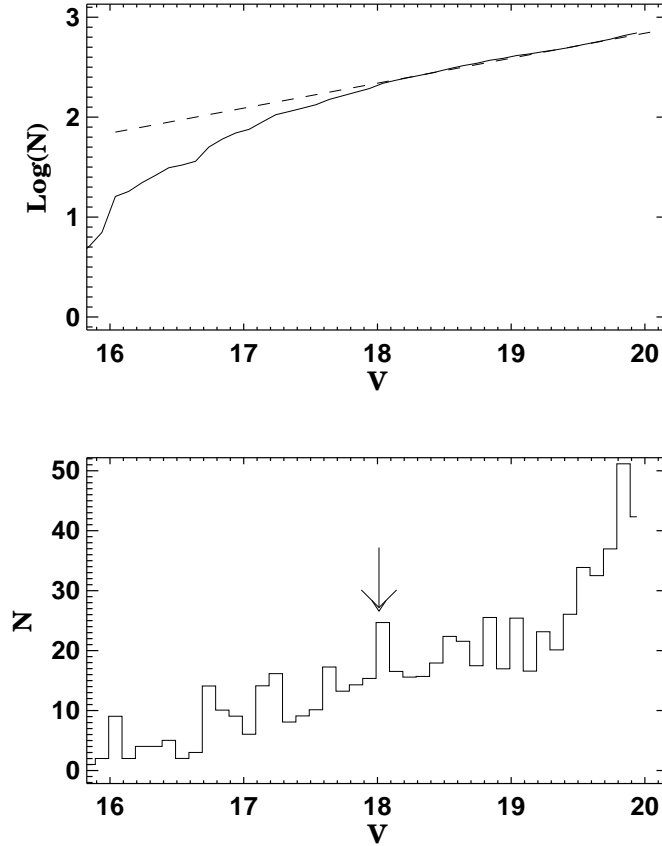
Fig. 7.— The observed integrated (upper panel) and differential (lower panel) luminosity function for the NGC 6229 RGB. The arrow indicates the possible location of the RGB "bump" in the cluster. These plots should be compared with the similar ones presented by Fusi Pecci et al. (1990) for M3.

does not seem to be as sharp as those found for other clusters of similar metallicity (cf. Figs. 3 and 4 in Fusi Pecci et al., and Ferraro et al. 1996 for an updated discussion of the case of M3).

Finally, we have analyzed the width of the RGB of NGC 6229 for signs of an internal metallicity dispersion. The "intrinsic" width of the RGB was estimated on the basis of the Simoda & Tanikawa (1970) and Da Costa & Armandroff (1990) methods. The results are consistent with no internal metallicity dispersion in NGC 6229.

5. HB morphology

5.1.   Variable stars

The Third Catalog of Variable Stars in Globular Clusters (Sawyer Hogg 1973) lists 22 variable stars in NGC 6229. One of them (V8) is a Population II cepheid, another (V22) is probably a slow variable star, and the remaining objects are RR Lyrae-type variables. It is instructive to note that the presence of Population II cepheids is known to be restricted to GCs containing well-developed blue HBs only (Wallerstein 1970; Smith & Wehlau 1985). For this reason, the existence of even a single such star in NGC 6229 could have been used as a strong argument against the results of Cohen (1986), who had found the HB of NGC 6229 to be extremely red.

In their survey CFT91 have obtained the magnitudes and colors for 20 variable stars from Sawyer Hogg's (1973) catalog (cf. Table 2 in CFT91) and have found 1 possible variable star (their No. 155). On our frames only 8 variable stars from the Sawyer Hogg catalog were actually detected because of our small field of view: V5, V6, V8, V11, V12, V15, V16, and V20.

In order to search for as yet undetected variables, the method proposed by Kadla & Gerashchenko (1982) was used. Such a method is based on the determination of the positions of the RR Lyrae variables on a CMD obtained from measurements of two images taken within a time interval that is much shorter than the periods of the variables. Kadla & Gerashchenko's original application of the method was devoted to the GC M3, where the instability strip region is much more heavily populated than in NGC 6229. After obtaining B and V frames with a separation in time of only 10 min, they showed that the RR Lyrae stars occupied a quite well-defined region in the CMD (cf. their Fig. 1), with only minor overlap with the stable red and blue HB. New variable star candidates could then be detected, even without several different frames being available for the cluster, on the basis of their "instantaneous" positions on the CMD. It should be emphasized that, for the method to work properly, the B and V magnitudes *must* be measured at the same phase. This will, of course, ensure that the large majority of the RR Lyrae stars in such a CMD will be located within the RR Lyrae "gap."

In the case of NGC 6229, as already emphasized, not many known RR Lyrae variables are present in our observed field. However, as shown in Fig. 1, most of the 12 new RR Lyrae candidates obtained with the method stand out quite clearly in the CMD and are unlikely to be misidentifications. A second pair of B and V images that we have obtained to check this result again shows all of these 12 candidates to lie within the instability strip region. The star lying at $(V, B-V) \simeq (18.1, 0.42)$ has uncertain photometry in one of the two pairs of B, V images. From inspection of this plot and of Fig. 1 in Kadla & Gerashchenko (1982), we deem it highly unlikely that a significant number of RR Lyrae variable candidates has been missed in the present study.

Information about the new RR Lyrae candidates is given in Table 4. In columns 2 and 3 of this table, we list the coordinates (in $''$) of the suspected variables in the Sawyer Hogg (1973) system. The next two columns contain V and $B-V$ values, determined by only one image pair. $R_{\rm c}$ is the projected radial distance (in $'$) from the cluster center. We are currently undertaking a new program to check the variability of these objects and obtain detailed light curves for the

TABLE 4. Possible variable stars in the core of NGC 6229.[a]

Star number	X ($''$)	Y ($''$)	V	$B - V$	$R_{\rm c}$ ($'$)
1	−4.09	−7.30	18.47	0.46	0.13
2	+12.62	−2.55	18.18	0.45	0.20
3	−3.86	+4.64	17.90	0.36	0.20
4	+6.94	+11.54	17.29	0.34	0.21
5	−10.29	+7.76	18.56	0.44	0.24
6	−15.71	−0.91	18.40	0.34	0.29
7	−16.83	+7.77	17.57	0.15	0.34
8	−21.29	−4.03	18.12	0.45	0.40
9	+23.69	−7.10	18.22	0.43	0.40
10	+5.46	+27.49	18.17	0.44	0.44
11	+17.97	+28.72	18.18	0.42	0.54
12	+24.35	−22.02	18.18	0.42	0.52

[a]NGC 6229: $\alpha(1950) = 16^{\rm h}45^{\rm m}\!.6$, $\delta(1950) = +47°37'$

confirmed RR Lyraes.

5.2. Number counts

The HB of NGC 6229 reveals many interesting features. We confirm the finding by CFT91 that the HB morphology of NGC 6229 is peculiar and atypical for an outer-halo cluster. In particular, NGC 6229 displays a well-populated blue HB tail, extending to quite blue colors and to a faint luminosity level ($\simeq 2.5$ mag below the RR Lyrae level in V). The presence of such an extended blue HB tail is a very unusual property for an outer-halo GC, although it is consistent with the presence of a Population II cepheid in this cluster (cf. Sect. 5.1).

Using the combined list of stars from this work and from the CFT91 study, the number of detected HB stars has now been increased to 235, or 266 after applying a completeness correction. This is to be compared with the 87 HB stars previously studied by CFT91. Our study thus improves considerably the degree of statistical significance of the detected HB features.

Following Fusi Pecci et al. (1993), we have estimated the degree of "statistical significance" of the present sample of HB stars. We have calculated their parameter $\mathrm{Frac}_{\rm HB} = N_{\rm HB}^{\rm obs}/N_{\rm HB}^{\rm tot}$, where $N_{\rm HB}^{\rm obs}$ and $N_{\rm HB}^{\rm tot}$ are the observed and total number of HB stars, respectively, within the GC. The total number of stars expected to populate the HB of NGC 6229 is ≈ 250, according to Eq. (14) of Renzini & Buzzoni (1986), assuming $\log L_{\rm tot} \simeq 5.1$ [as obtained from the integrated V magnitude M_V listed by Harris (1996), and assuming $M_V \approx M_{\rm bol}$ (Fusi Pecci et al. 1993)]. The implied degree of statistical significance of the present sample is thus quite high, although it

TABLE 5. Number of stars in the different branches of the NGC 6229 CMD.

$B2$	B_W	Blue HB	RR Lyrae	Red HB	AGB	RGB	Comment
77	25	102	$7+12^{\mathrm{b}}$	69	37	178	Present work [a]
28	17	45	$11+1^{\mathrm{b}}$	17	14	59	CFT91 [c]
105	42	147	$18+12^{\mathrm{b}}+1^{\mathrm{b}}$	86	51	237	Present work + CFT91's data

[a]Corrected for completeness

[b]Possible variables

[c]Stars in common with our study have been ommited

should be noted that the total HB population cannot be accurately predicted in this way due to the uncertainties in, e.g., the "evolutionary flux," the cluster distance modulus, and the bolometric correction.

To determine the number of stars in the HB, RGB, and asymptotic giant branch (AGB) phases, we followed the procedure used by Buzzoni et al. (1983). The data were corrected for completeness and the estimated numbers rounded to the closest integer value. The results for the number of stars on the different branches of NGC 6229 are presented in Table 5. In this table, B_W represents the number of HB stars in the color range $-0.02 < (B-V)_0 < 0.18$, and $B2$ the number of HB stars bluer than $(B-V)_0 = -0.02$ (cf. Buonanno 1993). The data quoted from CFT91 do not include the 60 stars in common with our study. We have thus counted up separately the stars with $r_c < 1.5'$ from our data and with $r_c > 1.5'$ from the CFT91 data. We point out the uncertain photometry and the small number of measured stars within the central $15''$.

Such number counts may be employed to estimate several useful HB morphology parameters. One of the most traditional is the so-called Dickens (1972) type (DT). Harris (1996) has estimated a $DT = 3$ for NGC 6229, based on the CFT91 CMD. From Fig. 5 in Dickens' original paper, however, one clearly sees that such an HB morphology classification should correspond to a high density of stars within the instability strip, and to a significantly smaller number of stars on the blue HB and (especially) the red HB. However, the number counts for NGC 6229 show a relative deficit of RR Lyrae variables compared to the total HB population. From Table 5, one finds $B : V : R = 0.59 : 0.08 : 0.33$ (where B, V, and R stand for the relative number of blue HB stars, RR Lyrae variables, and red HB stars, respectively). The corresponding number ratios for the typical $DT = 3$ cluster M5 (NGC 5904) are $B : V : R = 0.56 : 0.24 : 0.20$, according to the compilation presented by Lee et al. (1994). For comparison, M3 (NGC 5272) has a $DT = 4$ HB with $B : V : R = 0.33 : 0.42 : 0.25$, and M92 (NGC 6341) has a quite blue $DT = 2$ HB, with $B : V : R = 0.90 : 0.08 : 0.02$. We thus conclude that the classification of NGC 6229 as a $DT \approx 3$ cluster is probably not correct.

Following Harris' (1996) classification scheme, and using the number counts in Table 5, we believe it would probably be more appropriate to identify this cluster as a $DT = (1 \pm 1)/(7 \pm 1)$ cluster—i.e., a cluster with a bimodal HB distribution, resembling those of NGC 2808 (Ferraro

et al. 1990: $DT = 0/7$, $B : V : R = 0.23 : 0.01 : 0.76$) or NGC 1851 (Walker 1992: $DT = 1/6$, $B : V : R = 0.28 : 0.11 : 0.61$), but with a larger relative population of blue HB stars than in these two other bimodal-HB clusters. Other good, but perhaps less well-known, bimodal-HB candidates are M4 (NGC 6121), with $B : V : R = 0.34 : 0.25 : 0.41$; NGC 6362, with $B : V : R = 0.19 : 0.04 : 0.77$; NGC 6723, with $B : V : R = 0.37 : 0.19 : 0.44$; and M75 (NGC 6864), with $B : V : R = 0.27 : 0.07 : 0.66$ (number counts are from Lee et al. 1994). None of these has been classified as a bimodal-HB cluster by Harris. A bimodal HB has been assigned to M62 (NGC 6266) by the latter author. However, Brocato et al. (1996) have very recently derived $B : V : R = 0.58 : 0.26 : 0.16$ for M62, thus ruling out a bimodal HB for the cluster. We will return to this question of bimodality in Sect. 5.3.

Table 6 lists a number of other parameters obtained from our number counts for NGC 6229. We include in this table the inferred values for several of the new HB morphology indicators that Fusi Pecci et al. (1993) and Buonanno (1993) have recently defined. The quantities listed in Table 6 are as follows: N_{HB} is the number of HB stars, N_{RGB} is the number of RGB stars brighter than the HB level, N_{AGB} is the number of AGB stars, $(B-V)_W$ is the derived mean color for stars falling in the range $-0.02 < (B - V)_0 < 0.18$, and $B_W = N_{-0.02<(B-V)_0<0.18}^{\mathrm{HB}}$ is the number of stars in this color interval. The values in parentheses are for the case when the suspected variable stars are included in the calculations. The errors were estimated on the basis of Poisson statistics.

The values derived for R of 1.00 ± 0.11 (using our data only) and 1.06 ± 0.10 (from all data) and R' of 0.83 ± 0.09 and 0.88 ± 0.08, respectively, are lower than average (Buzzoni et al. 1983). These parameters are sensitive to the envelope helium abundance in evolved GC stars, and their low values in NGC 6229 are suggestive of a lower-than-average envelope helium abundance [$Y \simeq 0.18$, according to Eqs. (11) and (12) in Buzzoni et al. (1983); see also CFT91], although alternative interpretations are possible (cf. Sweigart 1996). The suggestion by CFT91 that the apparently low helium abundance of NGC 6229 may be responsible for its relatively blue HB is not supported by HB evolutionary models, which instead predict that the HB morphology should get *redder* with decreasing Y (e.g., Sweigart 1987; Catelan 1993).

The values of R and R' would be affected by any incompleteness in the relevant number counts. However, for the R value in NGC 6229 to match the average value of 1.41 found by Buzzoni et al. (1983), we would have to have missed 71 HB stars or counted 50 RGB stars too many—requiring changes of $\approx 30\%$ and $\approx 24\%$, respectively, in the corresponding number counts. In the case of R', the corresponding changes are $\approx 33\%$ and $\approx 25\%$, respectively. However, as can be seen from Fig. 5, we have complete samples for AGB and RGB stars, and a completeness correction has been applied for the blue HB stars brighter than our photometric limit of $V \simeq 20.5$ mag. It is entirely possible that the blue HB tail in NGC 6229 extends to fainter magnitudes, in which case our number counts could be missing a significant number of very blue HB stars (see Sect. 5.4).

The ratios $R1$ and $R2$ have been used to confirm the existence of semiconvective zones outside

TABLE 6. Calculated parameters from the NGC 6229 CMD.

Parameters	Present work	CFT91	Present work + CFT91
$B/(B+R)$	0.59	0.73	0.63
	$\sigma = 0.10$	$\sigma = 0.21$	$\sigma = 0.09$
$(B-R)/(B+V+R)$	0.18 (0.17)	0.38 (0.38)	0.24 (0.23)
	$\sigma = 0.02$	$\sigma = 0.07$	$\sigma = 0.02$
$(B2-R)/(B+V+R)$	0.05 (0.05)	0.15 (0.15)	0.08 (0.08)
	$\sigma = 0.01$	$\sigma = 0.03$	$\sigma = 0.01$
B_W/B	0.25	0.38	0.29
	$\sigma = 0.06$	$\sigma = 0.11$	$\sigma = 0.05$
$(B-V)_W$	0.067	0.067	0.067
	$\sigma = 0.05$	$\sigma = 0.05$	$\sigma = 0.05$
$R = N_{\mathrm{HB}}/N_{\mathrm{RGB}}$	1.00 (1.07)	1.24 (1.25)	1.06 (1.12)
	$\sigma = 0.11$	$\sigma = 0.22$	$\sigma = 0.10$
$R' = N_{\mathrm{HB}}/N_{(\mathrm{RGB+AGB})}$	0.83 (0.89)	1.00 (1.01)	0.88 (0.92)
	$\sigma = 0.09$	$\sigma = 0.17$	$\sigma = 0.08$
$R1 = N_{\mathrm{AGB}}/N_{\mathrm{RGB}}$	0.22	0.24	0.21
	$\sigma = 0.04$	$\sigma = 0.07$	$\sigma = 0.04$
$R2 = N_{\mathrm{AGB}}/N_{\mathrm{HB}}$	0.21 (0.21)	0.19 (0.19)	0.20 (0.19)
	$\sigma = 0.04$	$\sigma = 0.06$	$\sigma = 0.03$

the helium-burning convective cores of HB stars (Renzini & Fusi Pecci 1988). The $R1$ ratio for NGC 6229 is similar to the one found by Buzzoni et al. (1983) for their sample of clusters ($\langle R1 \rangle = 0.21 \pm 0.03$), while the $R2$ ratio seems somewhat higher than average ($\langle R2 \rangle = 0.15 \pm 0.03$; Buzzoni et al. 1983). This result might be another indication that faint blue HB stars ($V \gtrsim 20.5$ mag) have been missed in our number counts.

5.3. Bimodality

There is a clear indication of a bimodal distribution in color along the HB of NGC 6229. A well-populated red HB and an extended blue HB tail are clearly present, but the instability strip level seems to be more scarcely populated. The Sawyer Hogg (1973) catalog lists 20 RR Lyrae stars. To this number should be added the one possible RR Lyrae star found by CFT91 and the 12 new possible RR Lyrae stars found in the present study within the central field of the cluster.
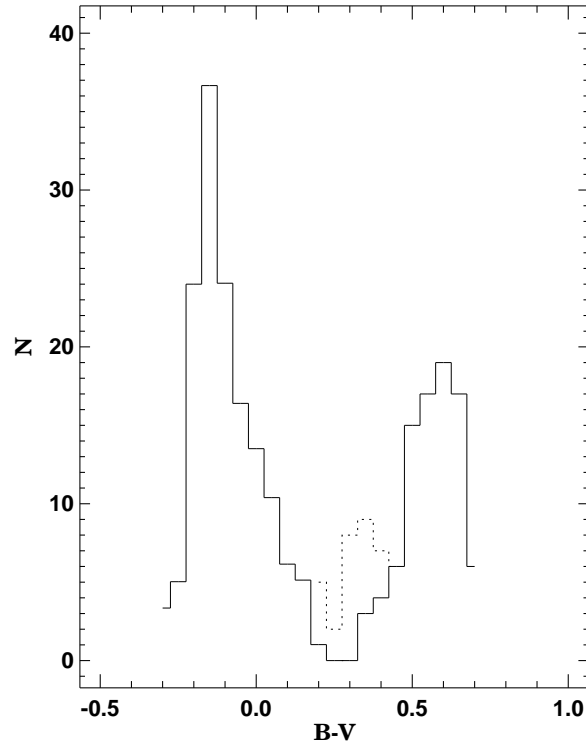
Fig. 8.— The histogram showing the color distribution of HB stars. The approximate distribution of the RR Lyrae stars is shown as dashed lines.

In order to estimate how many RR Lyrae stars may have been missed in our observational survey, we have carried out some numerical experiments. Our frames were taken "simultaneously" in B and V, thus ensuring that the instantaneous colors of the vast majority of the RR Lyrae stars would place them in the RR Lyrae gap (Kadla & Gerashchenko 1982; cf. Sect. 5.1). As in the completeness analysis (cf. Sect. 3.4), 30 artificial RR Lyrae stars with V magnitudes between 18.20 and 17.80 and B magnitudes between 18.25 and 18.65 were randomly added on the original images. The frames were then re-reduced as described in Sects. 2 and 3. The mean recovery efficiency was 87%, and the maximum number of "missing" RR Lyrae stars, in such experiments, was 7 (implying a recovery efficiency of $\simeq 77\%$).

The histogram showing the color distribution of HB stars is given in Fig. 8. The approximate distribution of the RR Lyrae stars is shown with dashed lines and corresponds to 33 RR Lyrae stars with "mean" colors randomly chosen so as to place them within the instability strip. Since NGC 6229 has been classified as an Oosterhoff type I cluster (Castellani & Quarta 1987), from the corresponding properties of fundamental and first-overtone pulsators we estimate that the 12 possible new RR Lyrae stars should be divided into ≈ 3 RRc and ≈ 9 RRab stars. Further photometry based on more images is necessary to obtain modern light curves for the RR Lyrae stars, confirm the nature of the newly identified RR Lyrae candidates, and check for the possible

presence of any as-yet unidentified variables (cf. Sect. 5.1).

It is also worth mentioning that the red extreme of NGC 6229's blue HB seems to be slightly brighter than the main part of the red HB of the cluster (cf. Figs. 1 and 2). The comparison with the more horizontal HB of M3 (cf. Fig. 6) makes this point especially clear. Stetson et al. (1996) have suggested that a similar effect may be present in the bimodal-HB clusters NGC 1851 and NGC 2808, with potentially important implications for age determinations using the "ΔV" method [cf. Eq. (1) in Catelan & de Freitas Pacheco (1995) and the accompanying discussion], and hence for our understanding of the second-parameter phenomenon. We will discuss these points more thoroughly in our subsequent paper (Catelan et al. 1996).

5.4.   Blue tail and "gaps"

CFT91 noted the possible presence of two gaps in the blue part of the HB, at $V \simeq 18.4$ mag and $V \simeq 19.7$ mag. The existence of the first gap is quite evident in the CMD (cf. Figs. 1 and 2). The reality of the second gap remains more elusive. The luminosity function of the blue HB stars gives support to the existence of two gaps, but more data extending to fainter magnitudes are clearly needed to settle the issue.

It should be remarked that the presence (or otherwise) of blue-HB stars fainter than $V \simeq 20.5$ mag in NGC 6229 remains quite uncertain. In the bimodal-HB cluster NGC 2808, for instance, Djorgovski et al. (1996) have recently found the blue HB tail to extend to magnitudes fainter than the main-sequence turnoff. If similar stars were present in NGC 6229, we would not have been able to detect them directly. However, the existence of a NGC 2808–like extended blue HB tail in NGC 6229 would increase the derived number ratios R and R' and decrease the ratio $R2$, compared to the values in Table 6, while keeping the ratio $R1$ unchanged. This is just the sense of the difference between our derived number ratios for NGC 6229 and the corresponding values for other clusters. An interesting analogy is provided by the core-concentrated cluster M80 (NGC 6093) (cf. Desidera 1996). Although the CFT91 photometry has a fainter threshold than the present one, it can probably still not rule out the presence of an extended blue HB tail. We recall that Ferraro et al. (1990, especially their Sect. 3.1) were not able to find good evidence for the surprisingly long NGC 2808 blue HB tail that has only very recently been detected by Djorgovski et al. from deep *HST* images of the cluster.

We conclude that deeper, high-quality photometry for NGC 6229 is urgently needed to show whether a very long, NGC 2808–like blue HB tail is present or not.
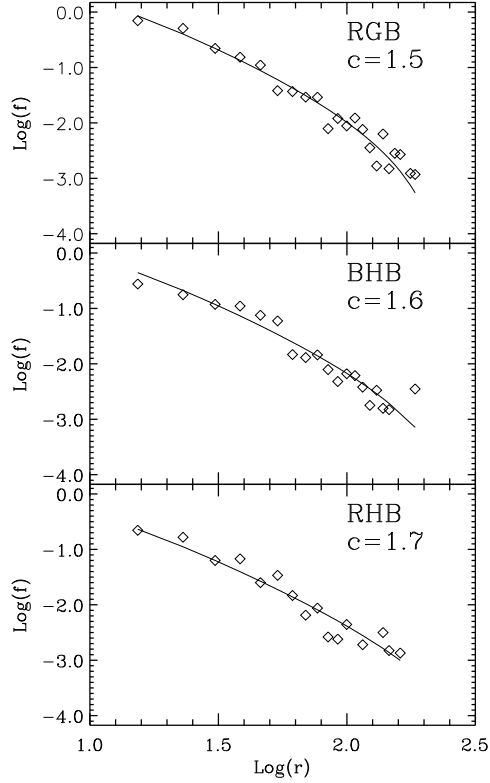
Fig. 9.— The observed radial distribution of RGB stars (upper panel), blue HB stars (middle panel), and red HB stars (lower panel). The best fitting King model with the indicated concentration parameter c is plotted for each distribution. "f" is the number of stars per squared radial bins, and the values are normalized to the maxima of the corresponding distributions. The distance r from the cluster center is given in ″. In these plots, the innermost points were omitted, because of poor statistics.

6. Radial distribution

The center of NGC 6229 was determined following the procedure outlined by Mateo et al. (1986). According to this technique, the cluster center is located at $X = 207.5 \pm 1.3$ px and $Y = 84.9 \pm 1.9$ px.

The structure of NGC 6229 was studied following King's (1966) iterative method by counting stars in concentric rings of increasing radii on the V image. The data were corrected with regard to the geometrical completeness of the annuli used. The standard χ^2 minimization procedures were used to fit the theoretical curves representing self-consistent King's dynamical models of star clusters. The best fit is consistent with $r_c = (7.9 \pm 2.3)''$ and $c = 1.60$. These values are in excellent agreement with those presented by Trager et al. (1993).
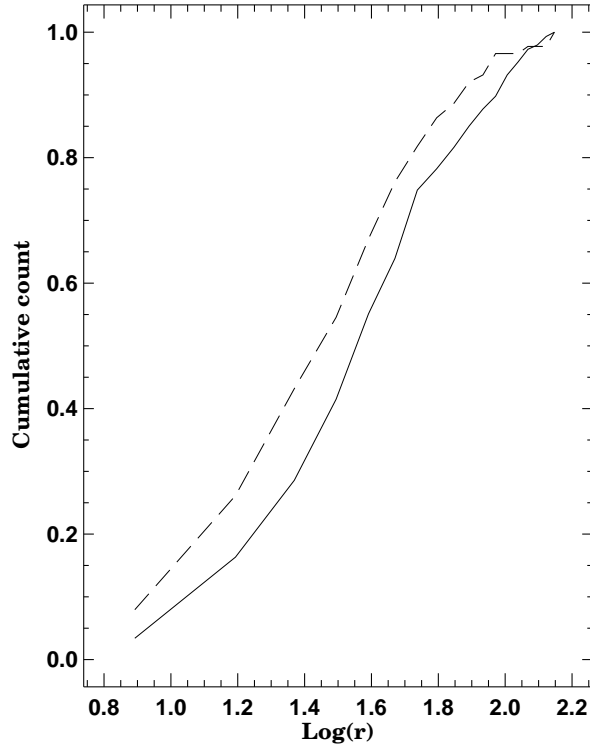
Fig. 10.— Radial cumulative distribution of blue HB stars (solid line) and red HB stars (dashed line) as a function of the projected distance from the cluster center (given in $''$).

In order to investigate the presence of radial population gradients, number counts were separately made for different components of the CMD (RGB, blue HB, and red HB) as a function of the radial distance from the cluster center. Different sets of theoretical King (1966) models were then computed for different values of the concentration parameter c. For this purpose, the observed surface brightness profiles were derived in concentric rings of increasing radii on the V image. A Kolmogorov-Smirnov test was applied to infer the best fit between theoretical and observed surface brightness profiles. The results are shown in Fig. 9, where c is the best-fit King concentration parameter for the corresponding subsample. As can be seen, the red HB stars are more strongly concentrated toward the cluster center, in comparison with the blue HB stars and the RGB population.

A second approach for investigating the radial population gradients involved a comparison of the cumulative radial distributions of stars in the blue and red portions of the HB. A Kolmogorov-Smirnov test applied to these two radial distributions, which are plotted in Fig. 10, yields a probability of 94.5% that they are different, again suggesting that the red HB stars are significantly more centrally concentrated than the blue HB population.

Following the method described by Buonanno et al. (1991), we have divided the HB stars in

two samples with equal number of stars—one including the stars lying inside the circle with radius $r = 0.59'$ and another including the stars lying outside this circle. We have then calculated the HB morphology index $(B - R)/(B + V + R)$ for these two regions separately. The resulting values are $(B - R)/(B + V + R) = 0.16 \pm 0.02$ for the inner region and $(B - R)/(B + V + R) = 0.31 \pm 0.02$ for the outer one. In other words, the mean color of the HB in the inner region appears to be shifted towards the red, compared to the outer region.

These radial trends in HB morphology, if real, are at least in qualitative agreement with those previously found for M15 = NGC 7078 (Stetson 1991b) and NGC 6752 (Buonanno et al. 1986). We caution, however, that deeper photometry is needed to detect any possible missing faint blue HB stars, especially near the cluster center. For additional information on radial population gradients in GCs, we refer the reader to the excellent discussions presented by Buonanno et al. (1991), Djorgovski et al. (1991), Djorgovski & Piotto (1992), and Stetson (1991b).

7.   Concluding remarks

Since the work by Sandage & Wildey (1967) on NGC 7006 and the analysis of the second-parameter phenomenon by Searle & Zinn (1978), it has become widely appreciated that clusters in the outer Galactic halo possess predominantly red HB morphologies. This has frequently been interpreted as a clue that the outer halo of the Galaxy may have taken longer to form than the inner halo (cf. Zinn 1993 for a recent discussion). The definition of "outer halo" has generally been based on studies of the spatial distribution of field RR Lyrae stars and halo GCs (e.g., Saha 1985; Zinn 1985; Carney et al. 1990). In particular, since the mass density–galactocentric distance relation for Galactic GCs presents a clear break at $R_{\rm GC} \simeq 20\,{\rm kpc}$ (cf. Fig. 10 in Carney et al. 1990), a dividing line between "regular" and "outer-halo" GCs which is independent of the HB morphology distribution of Galactic GCs has commonly been placed in the vicinity of 20 kpc (e.g., Ortolani 1987; CFT91), although different dividing lines which are not independent of HB morphology considerations have on occasion been used. In view of these arguments, and for consistency with CFT91, we will assume here, unless otherwise stated, that the Galactic outer halo begins at $R_{\rm GC} \simeq 24\,{\rm kpc}$.

Reasonably accurate CMD data are now available for some 13 outer-halo globulars. In Table 7, we summarize our present knowledge of the HB morphology for these outer-halo objects. The listed data [which also include the corresponding $R_{\rm GC}$, [Fe/H], c, M_V, and total estimated mass M of the cluster (obtained from M_V as in Djorgovski 1993)] have been obtained from the catalog by Harris (1996), to which we address the reader for the detailed references. For NGC 7006, we adopted the HB morphology provided by Buonanno et al. (1991). The outer-halo globular AM-4 ($R_{\rm GC} \simeq 24.2$ kpc, [Fe/H] $\simeq -2.0$, $M_V \simeq -1.5$; Harris 1996) has not been included due to the fact that it entirely lacks stars brighter than about the main-sequence turnoff (Inman & Carney 1987). From inspection of this table, one easily concludes that the standard view that outer-halo GCs possess predominantly red HB types is not valid. In fact, the number of outer-halo clusters with

TABLE 7. Some properties of the outer-halo GCs.

Cluster name	$(B-R)/(B+V+R)$	$R_{\rm GC}$ (kpc)	[Fe/H]	c	M_V	M ($10^4\,{\rm M}_\odot$)
	Red HBs					
Eridanus	−1.00	83.0	−1.46	1.10	−4.82	2.1
Pyxis	−1.00	37.0	−1.20	0.65	−5.59	4.3
Pal 4	−1.00	98.8	−1.48	0.78	−5.75	4.9
Pal 14	−1.00	64.9	−1.52	0.72	−4.60	1.7
AM-1	−0.93	117.2	−1.80	1.23	−4.60	1.7
Pal 3	−0.82	89.9	−1.66	1.00	−5.52	4.0
	Intermediate HBs					
NGC 7006	−0.11	36.9	−1.68	1.42	−7.58	26.6
Pal 13	−0.20	25.5	−1.79	0.66	−3.30	0.5
NGC 6229	+0.24	27.7	−1.44	1.60	−7.90	35.7
	Blue HBs					
NGC 5824	+0.82	26.0	−1.85	2.45	−8.88	88.1
NGC 2419	+0.86	97.7	−2.12	1.40	−9.48	153.2
Pal 15	+1.00	35.8	−1.90	0.60	−5.38	3.5
NGC 5694	+1.00	27.5	−1.86	1.84	−7.70	29.7

very blue HBs (4) is quite comparable to the number of outer-halo clusters with very red HBs (6). If one assumes that clusters with $20 \leq R_{\rm GC}({\rm kpc}) \leq 24$ are also outer-halo members, one may then even conclude that the outer halo has a predominantly *blue* HB (cf. Fig. 11): in this galactocentric distance range, all clusters listed by Harris (Arp 2, NGC 4147, NGC 5634, and NGC 7492) have blue HB types. In addition, one should be aware that, in the mean, the outer-halo clusters with bluer HB types seem to be significantly more luminous, and thus presumably also more massive, than those with redder HB types (Fig. 11d). From the masses presented in Table 7, one finds that the total mass contained in the six outer-halo clusters with red HBs is about *fifteen* times smaller than the total mass contained in the four outer-halo globulars with blue HBs, and even about 3.4 times smaller than the mass in the form of intermediate-HB clusters. Thus, if these GCs are representative survivors of the larger protogalactic fragments that may have led to the formation of the Galaxy (Searle & Zinn 1978; Zinn 1993), it is but reasonable to conclude that a more substantial fraction of the mass contributed by these fragments to the outer Galactic stellar halo was associated with stellar populations with predominantly *blue*, and *not* red, HB types—contrary to the usual assumption. In fact, if the outer-halo field population originated from dissolved GCs similar to the ones currently found there, its HB morphology would clearly be very blue.

We do confirm the trend discussed by CFT91 that the outer-halo clusters with redder HB types tend to have higher metallicities and be located farther away from the Galactic center, in comparison with the outer-halo clusters with bluer HBs (cf. Figs. 11a and 11b). In particular,
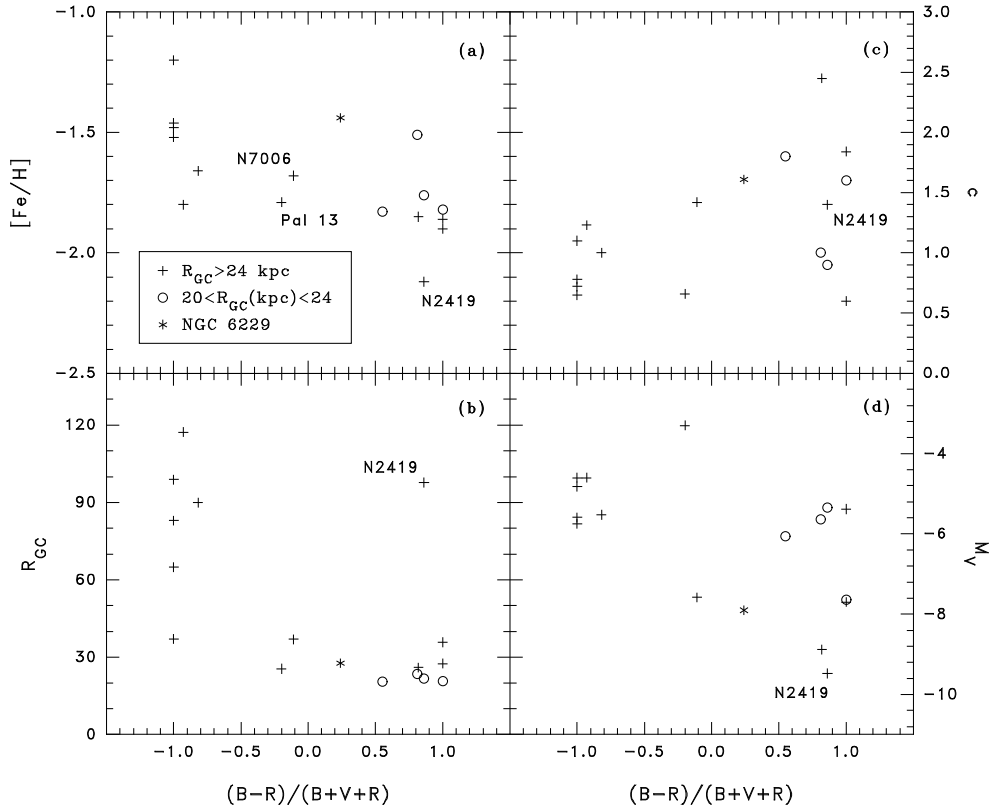
Fig. 11.— The HB morphology of outer-halo GCs, as a function of the metallicity (a); the Galactocentric distance (b), given in kpc; the central concentration c (c); and the integrated visual magnitude M_V (d). For NGC 5634, with $DT = 1$ (Harris 1996), we have assumed $(B - R)/(B + V + R) = +1$. Note that NGC 2419 is much more massive than the GCs with redder HB types lying at comparable galactocentric distances.

outside $R_{GC} = 40$ kpc, five out of six clusters seem to possess red HB types. However, the cluster with a blue HB that is found in this region, NGC 2419, is *much* more massive than any of the red-HB clusters lying at comparable galactocentric distances (cf. Fig. 11d and Table 7). Racine & Harris (1975) have argued that NGC 2419 may have a relatively small ($\simeq 24$ kpc) perigalactic distance, and currently be near its apogalacticon. If this cluster formed near its perigalacticon—a possibility that Racine & Harris advocate—its peculiar position among the remainder of the outer-halo globulars with $R_{GC} > 40$ kpc in Fig. 11b might then perhaps not seem so surprising, once we recall van den Bergh's (1995) remark that cluster properties tend to correlate more strongly with their perigalactic distances than with their current distances from the Galactic center. This shows the importance of obtaining accurate orbits for the Galactic GCs.

At any rate, based on an inspection of Table 7 and Fig. 11a, and ignoring for the moment the difference in masses among the outer-halo globulars, we would like to advance the suggestion that a prominent characteristic of the outer-halo system of GCs, as far as the HB morphology

is concerned, is the paucity of objects with intermediate HB morphology types. In other words, we find a hint that the HB morphology distribution of the *ensemble* of outer-halo GCs seems to be bimodal itself. Apparently, the formation of clusters with *either very red or very blue* HB types was favored in the Galactic outer halo. NGC 7006 seems to be the only well-established example of a distant ($R_{\rm GC} \geq 20$ kpc) cluster with a more-or-less evenly populated HB ($B : V : R = 0.28 : 0.33 : 0.39$) known to date. Pal 13 also has an intermediate HB type, but the HB morphology is based on only 5 detected HB stars (Ortolani et al. 1985; Borissova et al. 1996). NGC 6229, on the other hand, has a very peculiar CMD, in the sense that it is the only outer-halo cluster with a bimodal HB and an extended blue HB tail. In fact, inspection of the published CMDs for the outer-halo, blue-HB clusters in Table 7 (NGC 5694: Ortolani & Gratton 1990; Pal 15: Harris 1991; NGC 2419: Christian & Heasley 1988; NGC 5824: Canon et al. 1990) confirms that none possesses as extended a blue HB as does NGC 6229.

Figs. 11c and 11d also suggest a significant correlation between the HB morphology and the central concentration c and integrated luminosity M_V. The correlations are definitely more significant than found by Lee et al. (1994) in their Fig. 8. The possibility that the cluster environment may affect the HB morphology has been discussed at considerable length by Fusi Pecci et al. (1993, 1996), Djorgovski et al. (1991), Djorgovski & Piotto (1992), van den Bergh & Morris (1993), and Buonanno et al. (1996).

Age estimates have also been published quite recently for several of the outer-halo globulars, allowing a test of the Searle & Zinn (1978) hypothesis that the red HBs of some of these objects (cf. Table 7) are due to lower-than-average ages. In the studies of the CMD properties of Pal 4 and Pal 14 by Christian & Heasley (1986) and Holland & Harris (1992), respectively, evidence was presented that they probably have "normal" ages, in comparison with the clusters of the inner halo (but see Armandroff et al. 1992 for a different point of view). This idea has received support in the recent investigation by Richer et al. (1996), who found that the ages of the outer-halo clusters Pal 3, Pal 4, NGC 2419, and NGC 6229 are very similar to those of the inner-halo objects in their sample. On the other hand, Sarajedini (1996) has recently challenged Holland & Harris' results for Pal 14, and Sarajedini & Geisler (1996) have suggested that Pyxis is probably another example of a "young" GC with a red HB. Thus, the Searle & Zinn concept that the ages of the outer-halo clusters should be substantially lower than the ages of the inner-halo clusters remains very controversial.

NGC 6229 may potentially play an important rôle in deciding what parameter(s), besides [Fe/H], control(s) the HB morphology for the outer-halo GCs. Since this appears to be the only outer-halo cluster that contains *both a blue and a red HB*, any successful explanation for the origin of this HB bimodality might in principle (cf. Rood et al. 1993; Stetson et al. 1996) also prove successful in explaining why the distribution of HB types for the outer-halo globulars appears to be bimodal as well. As already noted, however, the blue HB of NGC 6229 appears to be much more extended than in any other outer-halo globular studied to date, which may perhaps suggest a physically different origin for it, or an internal mechanism responsible for "spreading" the blue

HB of NGC 6229 towards hotter temperatures (Buonanno et al. 1996).

Finally, we would like to add a caveat. From inspection of the orbital properties of the outer-halo GCs, as recently provided by van den Bergh (1993, 1995), we find that most of the clusters listed in Table 7 have plunging orbits with respect to the Galactic center. Information on the shape of the orbit is presently lacking for Pyxis and Pal 15. AM-1 and NGC 6229 have uncertain orbital shapes. Also, the perigalactic distances of most of these globulars appear to exceed 9 kpc (again, information on this property is missing for the newly-discovered Pyxis cluster). NGC 6229, on the other hand, seems to have a perigalactic distance as small as 4.2 kpc (a similar value is found for NGC 5694 as well). It should thus be exceedingly important to refine the orbital characteristics for NGC 6229, so that its identification as a genuine member of the Galactic outer halo can be either firmly established or ruled out. In either case, NGC 6229, together with such clusters as NGC 1851 and NGC 2808, remains an exciting challenge to stellar structure and evolution models.

REFERENCES

Armandroff, T. E., Da Costa, G. S., & Zinn, R. 1992, AJ, 104, 164

Aurière, M., & Coupinot, G. 1989, in Proceedings of the 1st ESO/ST-ECF Data Analysis Workshop, edited by P. J. Grosbøl, F. Murtagh, and R. H. Warmels (ESO, Garching), p. 101

Bahcall, J. N., & Soneira, R. M. 1980, ApJS, 44, 173

Borissova, J., Markov, H., & Spassova, N. 1996, A&AS, in press

Brocato, E., Buonanno, R., Malakhova, Y., & Piersimoni, A. M. 1996, A&A, 311, 778

Buonanno, R. 1993, in The Globular Cluster–Galaxy Connection, ASP Conf. Ser. Vol. 48, edited by G. H. Smith and J. P. Brodie (ASP, San Francisco), p. 131

Buonanno, R., Caloi, V., Castellani, V., Corsi, C., Fusi Pecci, F., & Gratton, R. 1986, A&AS, 66, 79

Buonanno, R., Corsi, C. E., Bellazzini, M., Ferraro, F. R., & Fusi Pecci, F. 1996, AJ, submitted

Buonanno, R., Corsi, C. E., Buzzoni, A., Cacciari, C., Ferraro, F., & Fusi Pecci, F. 1994, A&A, 290, 69

Buonanno, R., Corsi, C. E., Pulone, L., Fusi Pecci, F., Richer, H. B., & Fahlman, G. C. 1995, AJ, 109, 663

Buonanno, R., Fusi Pecci, F., Cappellaro, E., Ortolani, S., Richtler, T., & Geyer, E. H. 1991, AJ, 102, 1005

Buzzoni, A., Fusi Pecci, F., Buonanno, R., & Corsi, C. 1983, A&A, 128, 94

Canon, R. D., Sagar, R., & Hawkins, M. R. S. 1990, MNRAS, 243, 151

Carney, B., Fullton, L., & Trammell, S. 1991, AJ, 101, 1699 (CFT91)

Carney, B., Latham, D. W., & Laird, J. B. 1990, AJ, 99, 572

Carretta, E., & Gratton, R. 1996, A&AS, in press

Castellani, V., & Quarta, M. L. 1987, A&AS, 71, 1

Catelan, M. 1993, A&AS, 98, 547

Catelan, M., Borissova, J., Sweigart, A. V., & Spassova, N. 1996, in preparation

Catelan, M., & de Freitas Pacheco, J. A. 1995, A&A, 297, 345

Christian, C., Adams, M., Barnes, J. V., Hayes, D. S., Siegel, M., Butcher, H., & Mould, J. R. 1985, PASP, 97, 363

Christian, C., & Heasley, J. 1986, ApJ, 303, 216 lo

Christian, C., & Heasley, J. 1988, AJ, 95, 1422

Cohen, J. 1986, AJ, 90, 2254

Coupinot, G., Hecquet, J., Aurière, M., & Futaully, R. 1992, A&A, 259, 701

Da Costa, G. S., & Armandroff, T. E. 1990, AJ, 100, 162

Desidera, S. 1996, Studio delle Stelle Evolute negli Ammassi Globulari Galattici, Tesi di Laurea (Università degli Studi di Padova, Padova)

Dickens, R. J. 1972, MNRAS, 157, 281

Djorgovski, S. 1993, in Structure and Dynamics of Globular Clusters, ASP Conf. Ser. Vol. 50, edited by S. Djorgovski and G. Meylan (ASP, San Francisco), p. 373

Djorgovski, S., & Piotto, G. 1992, AJ, 104, 2112

Djorgovski, S., Piotto, G., Phinney, E. S., & Chernoff, D. F. 1991, ApJ, 372, L41

Djorgovski, S., Sosin, C., Piotto, G., King, I. R., Dorman, B., Liebert, J., Renzini, A., & Rich, R. M. 1996, in Advances in Stellar Evolution, edited by R. T. Rood and A. Renzini (Cambridge University Press, Cambridge), in press

Ferraro, F. R., Carretta, E., Corsi, C. E., Fusi Pecci, F., Cacciari, C., Buonanno, R., Paltrinieri, B., & Hamilton, D. 1996, A&A, in press

Ferraro, F. R., Clementini, G., Fusi Pecci, F., Buonanno, R., & Alcaino, G. 1990, A&AS, 84, 59

Fusi Pecci, F., Bellazzini, M., Ferraro, F. R., Buonanno, R., & Corsi, C. E. 1996, in Formation of the Galactic Halo....Inside and Out, ASP Conf. Ser. Vol. 92, edited by H. Morrisson and A. Sarajedini (ASP, San Francisco), p. 221

Fusi Pecci, F., Ferraro, F. R., Bellazzini, M., Djorgovski, S., Piotto, G., & Buonanno, R. 1993, AJ, 105, 1145

Fusi Pecci, F., Ferraro, F. R., Crocker, D. A., Rood, R. T., & Buonanno, R. 1990, A&A, 238, 95

Harris, W. E. 1991, AJ, 102, 1348

Harris, W. E. 1996, AJ, 112, 1487

Holland, S., & Harris, W. E. 1992, AJ, 103, 131

Inman, R. T., & Carney, B. W. 1987, AJ, 93, 1166

Kadla, Z., & Gerashchenko, A. 1982, Izv. Main A. O. of the Academy of Sc. USSR (Pulkovo), 199, 86

King, I. 1966, AJ, 71, 64

Kraft, R. P., Sneden, C., Langer, G. E., & Prosser, C. F. 1992, AJ, 104, 645

Lee, Y.-W., Demarque, P., & Zinn, R. 1994, ApJ, 423, 248

Mateo, M. 1988, ApJ, 331, 261

Mateo, M., Hodge, P., & Schommer, R. 1986, ApJ, 311, 113

Murtagh, F., Starck, J.-L., & Bijaoui, A. 1995, A&AS, 112, 179

Ortolani, S. 1987, in Stellar Evolution and Dynamics in the Outer Halo of the Galaxy, ESO Conf. and Workshop Proc. No. 27, edited by M. Azzopardi and F. Matteucci (ESO, Garching), p. 341

Ortolani, S., & Gratton, R. 1990, A&AS, 82, 71

Ortolani, S., Rosino, L., & Sandage, A. 1985, AJ, 90, 473

Racine, R., & Harris, W. E. 1975, ApJ, 196, 413

Ratnatunga, K., & Bahcall, J. 1985, ApJS, 58, 63

Renzini, A., & Buzzoni, A. 1986, in Spectral Evolution of Galaxies, edited by C. Chiosi and A. Renzini (Reidel, Dordrecht), p. 195

Renzini, A., & Fusi Pecci, F. 1988, ARA&A, 26, 199

Richer, H. B., Harris, W. E., Fahlman, G. G., Bell, R. A., Bond, H. E., Hesser, J. E., Holland, S., Pryor, C., Stetson, P. B., VandenBerg, D. A., & van den Bergh, S. 1996, ApJ, 463, 602

Rood, R. T., Crocker, D. A., Fusi Pecci, F., Ferraro, F. R., Clementini, G., & Buonanno, R. 1993, in The Globular Cluster–Galaxy Connection, ASP Conf. Ser. Vol. 48, edited by G. H. Smith and J. P. Brodie (ASP, San Francisco), p. 218

Saha, A. 1985, ApJ, 289, 310

Sandage, A., & Wildey, R. 1967, ApJ, 150, 469

Sarajedini, A. 1996, AJ, in press

Sarajedini, A., & Geisler, D. 1996, AJ, 112, 2013

Saviane, I., Piotto, G., Zaggia, S., Fagotto, F., Capaccioli, M., & Aparicio, A. 1996, A&A, submitted

Sawyer Hogg, H. 1973, Publ. David Dunlap Obs., 3, No. 6

Searle, L., & Zinn, R. 1978, ApJ, 225, 357

Simoda, M., & Tanikawa, K. 1970, PASJ, 22, 143

Smith, H. A., & Wehlau, A. 1985, ApJ, 298, 572

Stetson, P. 1987, PASP, 99, 191

Stetson, P. 1991a, in The Formation and Evolution of Star Clusters, ASP Conf. Ser. Vol. 13, edited by K. A. Janes (ASP, San Francisco), p. 88

Stetson, P. 1991b, in Precision Photometry: Astrophysics of the Galaxy, edited by A. G. D. Philip, A. R. Upgren, and K. A. Janes (L. Davis Press, Schenectady), p. 69

Stetson, P. & Harris, W., 1988, AJ, 96, 909

Stetson, P., VandenBerg, D. A., & Bolte, M. 1996, PASP, 108, 560

Sweigart, A. V. 1987, ApJS, 65, 95

Sweigart, A. V. 1996, ApJ (Letters), in press

Trager, S., Djorgovski, S., & King, I. 1993, in Structure and Dynamics of Globular Clusters, ASP Conf. Ser. Vol. 50, edited by S. Djorgovski and G. Meylan (ASP, San Francisco), p. 347

van den Bergh, S. 1993, ApJ, 411, 178

van den Bergh, S. 1995, AJ, 110, 1171; erratum: AJ, 110, 3119

van den Bergh, S., & Morris, S. 1993, AJ, 106, 1853

Walker, A. 1992, PASP, 104, 1063

Wallerstein, G. 1970, ApJ, 160, 345

Zinn, R. 1985, ApJ, 293, 424

Zinn, R. 1993, in The Globular Cluster–Galaxy Connection, ASP Conf. Ser. Vol. 48, edited by G. H. Smith and J. P. Brodie (ASP, San Francisco), p. 38